An ultra-compact SSPP transmission line and its signal integrity analysis

Zi Hua You[1,2], Xin Xin Gao[1,2], Zhang Wen Cheng[1,2], Hai Lin Wang[1,2], Hui Feng Ma[1,2]*, and Tie Jun Cui[1,2]*

[1]*State Key Laboratory of Millimeter Waves, School of Information Science and Engineering, Southeast University, Nanjing 210096, China*

[2]*Institute of Electromagnetic Space, Southeast University, Nanjing, 210096, China*

[*]*Emails:* hfma@seu.edu.cn, tjcui@seu.edu.cn

Abstract

We propose an ultra-compact spoof surface plasmon polariton (UCSSPP) transmission line (TL) based on a meander line, which can achieve almost the same transmission performance as the conventional rectangular-groove SSPP TL, but the linewidth is greatly reduced by more than 40%. The coupling effect between two UCSSPP TLs in different line arrangements has been well studied, revealing that excellent crosstalk suppression can be achieved when two TLs are arranged back-to-back, while strong coupling occurs when they are arranged face-to-back or face-to-face. The signal integrity of back-to-back UCSSPP TLs is analyzed and demonstrated, which shows that the signal integrity can be greatly improved compared with microstrip (MS) TLs. In addition, based on the principle of mode mismatch, MS and UCSSPP TLs are arranged alternately to solve the mutual coupling problem in multi-line systems. On the other hand, benefiting from the strong coupling of face-to-face UCSSPP TLs, an ultra-miniaturized SSPP coupler working at 9 GHz is designed, whose size can be reduced by over 75% compared with conventional MS coupler. The measurement results show good agreement with full-wave simulations, indicating that the proposed UCSSPP TL has significant advantages in signal integrity and device miniaturization over previously reported SSPP TLs.

Index Terms – Spoof surface plasmon polariton, ultra-compact transmission lines, signal integrity, crosstalk suppression, miniaturized coupler

This article has been accepted for publication and undergone full peer review but has not been through the copyediting, typesetting, pagination and proofreading process, which may lead to differences between this version and the Version of Record. Please cite this article as doi: 10.1002/adem.202200621.

1. Introduction

Surface plasmon polaritons (SPPs) are electromagnetic (EM) surface waves propagating along the interface between conductor and dielectric at optical frequencies, which are tightly confined to the metal surface in the direction of propagation and decay rapidly in the plane perpendicular to the direction of propagation. SPPs have excellent physical characteristics such as strong field confinement and controllable transmission dispersion.[1,2] However, at lower frequency bands (such as microwave and terahertz), where the metal behaves as a perfectly electrical conductor (PEC) rather than a plasmon, SPPs cannot propagate along the metal surface. In 2004, the concept of spoof SPPs (SSPPs) supported by a sub-wavelength periodic metal structure was first proposed at low frequencies, and SSPPs have similar characteristics to natural SPPs.[3] In previous works, most of the structures are three-dimensional (3D) volume structures, which are difficult to be integrated with planar circuits.[4-6] In 2013, an ultra-thin SSPP waveguide was proposed to support and propagate SSPPs mode on arbitrarily curved surfaces.[7] In 2014, a matching transition was proposed to realize high conversion efficiency between the guided waves and SSPPs.[8] Later, some gradient transition structures were used to achieve the impedance matching between the MS TL and SSPP TL,[9-12] which promote the research of SSPP devices to be integrated with microwave circuits.

In recent years, many SSPP devices, such as filters,[13-17] splitters,[18-21] frequency dividers and couplers,[22-24] leaky-wave antennas, [25-27] and SSPP systems,[28,29] have been reported, and some works to reduce the size of SSPP structure have also been proposed for miniaturization design of circuits.[30-32] In addition to miniaturization, crosstalk suppression is always an important issue to be solved in highly integrated circuits. Thanks to the strong confinement characteristics of SSPPs, they have naturally exhibited unique advantages in crosstalk suppression.[33-36] However, most of the previously reported works either have a complicated double-layer structure that is difficult to be compatible with the conventional MS circuits or have wide linewidth that is not conducive to the design of highly integrated circuits. Hence, the development of TL with narrow linewidth and good signal integrity can realize the miniaturization of devices and greatly improve the degree of integration of planar circuits.

In this paper, we propose an ultra-compact SSPP (UCSSPP) TL based on a meander line structure, which can achieve almost the same transmission performance as the conventional rectangular-groove SSPP TL, while the linewidth is reduced by 42%. Considering the asymmetry of UCSSPP structure,

the mutual coupling with different line arrangements between two UCSSPP TLs has been discussed. It is revealed that excellent crosstalk suppression can be achieved when two TLs are arranged back-to-back, while strong mutual coupling occurs in both face-to-back and face-to-face arrangements. In addition, based on the principle of mode mismatch, UCSSPP and MS TLs can be alternately arranged to achieve crosstalk suppression in multi-wire system. On the other hand, taking the advantage of the strong coupling of UCSSPP TLs in face-to-face arrangement, an ultra-compact coupler with cross-transmission function is designed, fabricated and measured, which shows almost the same good coupling performance as the conventional MS coupler, but the size can be reduced by over 75%. Since the proposed UCSSPP TL can achieve good field confinement within ultra-narrow linewidth, and the propagation constant can be flexibly controlled by adjusting its geometric parameters, which may find great potential application value in modern high-speed and high-density integrated circuits.

2. Design of UCSSPP TL

Figure 1a,b,c shows unit structures of three different TLs, in which Figure 1a is the conventional MS TL, Figure 1b is the conventional SSPP TL, and Figure 1c is the proposed UCSSPP TL, respectively. These unit structures are supported by a grounded dielectric substrate of F4BM220 with relative permittivity of 2.2, tangential loss of 0.001, and thickness of t_s = 0.508 mm. The yellow parts of the upper and lower layers are copper with a conductivity of 5.8×10^7 S/m and a thickness of 0.018 mm. The other parameters shown in Figure 1a,b,c are a = 0.9 mm, g = 0.3 mm, and h_m, h_s, h_u, d_s, d_u are variables. Figure 1d shows the dispersion curves of different units with the same period of p = 2.4 mm. The dispersion curves of SSPP units gradually deviate from the light line and MS line, and then approach different asymptotic frequencies. When these three units have the same linewidth, such as $h_m = h_s = h_u$ = 1.8 mm, the dispersion curve of UCSSPP structure (l = 2.1 mm, d_u = 1.2 mm) deviates more significantly than those of MS structure and conventional SSPP structure (d_s = 1.4 mm), which is because the current path is greatly extended due to the design of meander line, resulting in the significant increase of propagation wave number at a certain frequency. In order to obtain the same dispersion curve as that of UCSSPP structure, the linewidth of conventional SSPP unit needs to be increased to h_s = 3.1 mm (d_s = 2.7 mm), as shown in Figure 1d with pink and green lines. Figure 1e demonstrates the dispersion curves of UCSSPP structure with different d_u and l_u. The results show that the asymptotic frequency and propagation constant can be flexibly adjusted by changing these

two parameters.

The transmission performance of both UCSSPP TL and conventional SSPP TL with the similar dispersion characteristics was compared by both full-wave simulations and experimental measurements, as shown in **Figure 2**. The photographs of experimental samples of UCSSPP TL and conventional SSPP TL are illustrated in Figure 2a,b, respectively. The TLs consist of three parts: the MS line transition section with the port impedance of 50 Ω (region 1), the MS-SSPP matching transition section (region 2), and the SSPP transmission section (region 3). The lengths of each part is L_1 = 12 mm, L_2 = 14.4 mm, L_3 = 28.8 mm, and the linewidth of 50 Ω MS port is w_0 = 1.5 mm. The parameters of the MS-SSPP matching transition section are optimized to make smooth mode conversion.[8,10,11] In SSPP transmission section, the dimensions of UCSSPP structure are selected as h_u = 1.8 mm and l = 2.1 mm, and the dimensions of conventional SSPP structure are selected as h_s = 3.1 mm and d_s = 2.7 mm, both of which have the similar dispersion curves, as shown in Figure 1d with green and pink lines, respectively. Figure 2c displays the simulated S parameters of two TLs, showing that they almost have the same transmission coefficient (S21), with the same cut-off frequency of 15.8 GHz, which is consistent with the dispersion curves shown in Figure 1d. In addition, compared with conventional SSPP TL, the reflection coefficient (S11) of UCSPP TL is much lower than that of conventional SSPP TL, because the UCSSPP TL has a similar linewidth with 50 Ω ports, which makes it easier to achieve a good impedance match. The measured results are generally in good agreement with the simulations, as shown in Figure 2d. However, it should be noted that the measured S21 is slightly lower than the simulated one, especially at high frequency band, which may be caused by excessive solder accumulation on the probe and shell during manual welding of SMA, resulting in limited working bandwidth of SMA and loss at high frequency. In addition, the minor errors of dielectric substrate parameters at high frequency also lead to the degradation of the transmission coefficient.

3. Analysis of the signal integrity

Since the UCSSPP TL is an asymmetry structure, we discussed the mutual coupling between two UCSSPP TLs lines under three different cases of A, B and C, i. e. back-to-back, face-to-face and face-to-back, as shown in **Figure 3**a. Each pair of transmission lines is composed of the MS transition part (region 1), the MS-SSPP conversion part (region 2) and the SSPP coupling part (region 3). The separation between two UCSSPP TLs in region 3 is s, and the coupling length is L_3. Figure 3b shows

the simulated transmission coefficient (S21) and coupling coefficient (S41) of these three cases when s = 0.4 mm and L_3 = 38.4 mm, where the power is fed from port1. The results show that the best crosstalk suppression between two UCSSPP TLs can be achieved by case A (back-to-back), whose S41 is below -16 dB in whole frequency band, while both cases B and C have significant mutual crosstalk. Figure 3c shows the simulated near-field distributions of electric fields on the cross section of the UCSSPP unit. The results demonstrate that the electric field is mainly concentrated on the "face" side of the structure, showing a strong field enhancement, while the electric-field energy on the "back" side of the structure is obviously weak. Therefore, only when two UCSSPP TLs are arranged back-to-back, there will be weak field coupling between two lines, and good crosstalk suppression can be achieved.

To demonstrate the performance of UCSSPP TL in crosstalk suppression, we make a comparison between UCSSPP TL (back-to-back) and MS TL, as shown in **Figure 4**. The simulation models of UCSSPP TL and MS TL are shown in Figure 4a,b, respectively, in which the separation between two TLs is s and the power is fed from port 1. The simulated S21 and S41 are illustrated in Figure 4c,d,e,f. The results show that both TLs have good transmission performance for different s, especially when s > 0.2 mm, as shown in Figure 4c,d. However, when s is gradually increased from 0.2 to 0.6 mm, the performance of crosstalk suppression becomes better and better based on UCSSPP TL, which can achieve -28 dB when s = 0.6 mm, as shown in Figure 4e, while crosstalk almost does not change for conventional MS TL, whose coupling interference remains at -10 dB from 8 to 12 GHz, as shown in Figure 4f. Hence, compared with the conventional MS TL, the better crosstalk suppression can be achieved by using the proposed UCSSPP TL in back-to-back case.

Figure 5a,b shows the simulated electric field distributions of z component on two UCSSPP and MS TLs at 11 GHz with the separation s = 0.6 mm. Compared with MS TL, the EM waves have shorter wavelength and stronger field confinement when propagating along the UCSSPP TL, and there is almost no mutual coupling between two adjacent TLs, as shown in Figure 5a, while the strong coupling occurs when EM waves propagate along the MS TL, as shown in Figure 5b. The cross-section electric field distributions of two TLs on the *yoz*-plane at 1.2mm along the x-direction from the middle position of the coupling part are demonstrated in Figure 5c,d, respectively, where the white dotted boxes are the positions of two TLs. It can be clearly seen that the electric fields are strictly confined on the primary line when propagating along UCSSPP TLs, but mutual interference is serious when propagating along MS TLs.

The closely arranged TLs with s = 0.3 mm and s = 0.6 mm are fabricated and measured, as illustrated in **Figure 6**, in which Figure 6a,b shows the photographs of UCSSPP TLs and MS TLs, respectively. The measured S21 and S41 for the cases of s = 0.3 mm and s = 0.6 mm are demonstrated in Figure 6c,d, respectively. The results show that compared with MS TLs, the S41 of UCSSPP TLs can be reduced by up to 10 dB and 20 dB when s = 0.3 mm and s = 0.6 mm, respectively.

The signal integrity of TLs with s = 0.6 mm is further analyzed by full-wave simulations, as shown in **Figure 7**. The time-domain input signals of broadband Gaussian pulses (8 −12 GHz) with 0.5 ns time intervals from port 1 and port 3, respectively, as shown in Figure 7a. The output signals of UCSSPP TL and MS TL from port 2 and port 4 are demonstrated in Figure 7b,c, respectively. The results show that the signals are nearly distortionless after passing through two close UCSSPP TLs, but significantly distorted after passing through two close MS TLs, which further proves the better crosstalk suppression of UCSSPP TLs.

Considering that UCSSPP TLs can achieve good crosstalk suppression when arranged back-to-back, they can be used to solve the signal integrity problem of two-wire system, but cannot be applied to multi-wire system, such as three or more closely arranged TLs. In order to solve this problem, the mode mismatch method may be a good choice to achieve low crosstalk by alternately arranging the UCSSPP TL and MS TL.[28] Figure 8a,b shows two different arrangements of UCSSPP TL and MS TL, named Case-1 and Case-2, respectively. The simulated S21 and S41 of two cases with s = 0.1 mm, 0.3 mm and 0.5 mm are shown in Figure 8c,d, respectively. The results show that good S21 are achieved in a wide band for both cases, and the S41 all can keep at a low level, which are lower than -20 dB for Case-1 with s = 0.1 mm and Case-2 with s = 0.3 mm. **Figure 9**a,b shows the fabricated samples of Case-1 (s = 0.1 mm) and Case-2 (s = 0.3 mm), respectively, and the measured results of S21 and S41 are shown in Figure 9c, which are in good agreement with the simulations, indicating the good crosstalk suppression performance. Therefore, the alternate arrangement of UCSSPP and MS TLs is a good choice to realize low crosstalk transmission for multi-wire system. It is worth noting that there should be a phase delay between the output signals of two TLs due to the different propagation constants, but it is possible to be solved by extending the length of MS TL.

Compared to the previously reported works,[33-36] the proposed UCSSPP TL has narrower linewidth and can achieve better crosstalk suppression performance at a smaller separation, as summarized in Table 1.

4. Design of the compact SSPP Coupler

According to the above discussion, the proposed UCSSPP TLs have strong coupling when they are arranged by face-to-face, it is not conducive to crosstalk suppression, but can be adapted to the coupler design. Based on the coupled-mode theory, the transmitted power ratio (T) and coupling power ratio (C) of the adjacent waveguide system can be expressed as[37]

$$\begin{cases} T = \cos^2(\kappa L_3) e^{-2\alpha L_3} \\ C = \cos^2(\kappa L_3) e^{-2\alpha L_3} \end{cases} \quad (1)$$

where L_3 is the coupling length of TL, α is the imaginary part of the propagation constant, and κ is the frequency-dependent coupling coefficient.

Suppose that the power is fed from port 1, if all energy is required to output from the straight-through port (port 2), C should be equal to 0, then the coupling length L_3 is calculated as $L_3 = 2nL_0$, $n = 1, 2, 3\ldots$, where L_0 is defined as $L_0 = \frac{\pi}{2\kappa}$.[38] However, if all energy is required to output from the coupling port (port 4), T should be equal to 0, then the coupling length is calculated as $L_3 = 2(n\text{-}1)\,L_0$, $n = 1, 2, 3\ldots$. In addition, κ is positively correlated with the frequency f and separation s between two TLs, and inversely correlated with the coupling length L_3. Hence, a coupler with cross-transmission function at desired frequency f can be designed by adjusting s and L_3.

Here, we designed a coupler for cross-transmission at 9 GHz based on the proposed UCSSPP TLs, as shown in **Figure 10**a. The separation between two UCSSPP TLs is s = 0.2 mm, the coupling length is optimized as L_3 = 38.4 mm, and the linewidth is h_u = 1.8 mm. As a comparison, an MS coupler with the same linewidth h_m and separation s is also designed, as shown in Figure 10b. To make the MS coupler work at the same frequency of 9 GHz, the coupling length must be increased to L_3 = 170.4 mm, which is nearly 4.5 times of UCSSPP coupler. Figure 10c,d shows the electric field distributions of z component on the *xoy* plane at 9 GHz when the power is fed from port 1. As indicated, the input power of two couplers is almost fully coupled to the adjacent TL and outputs from port 4. The simulated S parameters are displayed in Figure 10e. The results show that both couplers almost have the similar S parameter curves, especially below 11 GHz, which demonstrate good coupling performance at 9 GHz. In addition, the size of the coupler can be further reduced by adjusting the geometric parameters of UCSSPP unit to increase the propagation constant. The inset in Figure 10e shows the S parameters of new designed UCSSPP coupler when the linewidth of UCSSPP structure is increased to h_u = 3.1 mm (d_u = 2.5 mm), as shown in Figure 1c. It shows that

the coupler also works at 9 GHz with good performance, but the coupling length L_3 is only 19.2 mm, which is half of the previous UCSSPP coupler with h_u = 1.8 mm. Hence, the dimension of UCSSPP coupler can be flexibly designed at a certain working frequency, on the other hand, the working frequency also can be flexibly designed under a certain dimension. **Figure 11**a illustrates the photos of the fabricated couplers with h_u = 1.8 mm. The measured results show that the UCSSPP coupler almost has the same EM response as the MS coupler but in a much smaller size, as shown in Figure 11b.

5. Conclusion

An UCSSPP TL based on the meander-line has been proposed in this work, which can achieve a compact size and a lower asymptotic frequency. The coupling between two UCSSPP TLs with different line arrangements has been well studied. Compared with MS TLs, the UCSSPP TLs have excellent crosstalk suppression and signal integrity when arranged back-to-back. On the other hand, a super miniaturized SSPP coupler for cross-transmission at 9 GHz has been designed by taking advantage of the strong coupling of UCSSPP in face-to-face arrangement, and its working frequency can be adjusted arbitrarily. In addition, the alternate arrangement of UCSSPP and MS TLs has been adopted to solve the mutual coupling issue in multi-line system. All the performances of UCSSPP have been verified by both simulations and experiments, which have good agreement with each other. The proposed UCSSPP TL can not only suppress crosstalk and improve signal integrity, but also can be used to design miniature microwave devices, which is of great significance and potential value in modern communication systems and equipment.

Acknowledgment

This work was supported by the National Key Research and Development Program of China (Grant Nos. 2017YFA0700200, 2017YFA0700201, and 2017YFA0700202), National Natural Science Foundation of China (62071117 and 61831006), the Major Project of the Natural Science Foundation of Jiangsu Province (BK20212002), the 111 Project (111-2-05), the Project for Jiangsu Specially-Appointed Professor, and the Six Talent Peaks Project in Jiangsu Province (XCL-077).

Conflict of Interest

The authors declare no conflict of interest.

Reference

1. W. L. Barnes, A. Dereux, T. W. Ebbesen, *Nature* **2003**, *424*, 824.
2. S. A. Maier, *Plasmonics: Fundamentals and Applications*, Springer, Berlin **2007**.
3. J. B. Pendry, L. Martin-Moreno, F. J. Garcia-Vidal, *Science* **2004**, *305*, 847.
4. A. P. Hibbins, B. R. Evans, J. R. Sambles, *Science* **2005**, *308*, 670.
5. F. J. Garcia-Vidal, L. Martin-Moreno, J. B. Pendry, *J. Opt. A: Pure Appl. Opt.* **2005**, *7*, S97.
6. W. S. Zhao, O. M. Eldaiki, R. X. Yang, Z. L. Lu, *Opt. Exp.* **2010,** *18*, 21498.
7. X. P. Shen, T. J. Cui, D. Martin-Cano, F. J. Garcia-Vidal, *Proc. Natl. Acad. Sci. U. S. A.* **2013**, *110*, 40.
8. H. F. Ma, X. P. Shen, Q. Cheng, W. X. Jiang, T. J. Cui, *Laser Photonics Rev.* **2014**, *8*, 146.
9. Z. Liao, J. Zhao, B. C. Pan, X. P. Shen, T. J. Cui, *J. Phys. D: Appl. Phys.* **2014**, *47*, 315103.
10. A. Kianinejad, Z. N. Chen, C. W. Qiu, *IEEE Trans. Microwave Theory Tech.* **2015,** *63*, 1817.
11. D. W. Zhang, K. Zhang, Q. Wu, R. Dai, X. J. Sha, *Opt. Lett.* **2018**, *43*, 3176.
12. D. W. Zhang, X. Liu, Y. X. Sun, K. Zhang, Q. Wu, Y. S. Li, T. Jiang, *Opt. Lett.* **2021**, *43*, 4354.
13. B. C. Pan, Z. Liao, J. Zhao, T. J. Cui, *Opt. Exp.* **2014**, *22*, 13940.
14. X. Gao, L. Zhou, Z. Liao, H. F. Ma, T. J. Cui, *Appl. Phys. Lett.* **2014**, *104*, 191603.
15. D. F. Guan, P. You, Q. F. Zhang, K. Xiao, S. W. Yong, *IEEE Trans. Microwave Theory Tech.* **2017**, *65*, 4925.
16. J. Wang, L. Zhao, Z. C. Hao, *IEEE Access* **2019**, *7*, 35089.
17. D. W. Zhang, Y. X. Sun, K. Zhang, Q. Wu, T. Jiang, *J. Phys. D: Appl. Phys.* **2022**, *55*, 165101.
18. X. Gao, L. Zhou, X. Y. Y u, W. P. Cao, H. O. Li, H. F. Ma, T. J. Cui, *Opt. Express* **2015**, *23*, 23270.
19. J. Wang, L. Zhao, Z. C. Hao, X. P. Shen, T. J. Cui, *Opt. Lett.* **2019,** *44*, 3374.
20. S. Y. Zhou, S. W. Wong, J. Y. Lin, L, Zhu, Y. J. He, Z. H. Tu, *IEEE Microw. Wireless Compon. Lett.* **2019**, *29*, 98.
21. Y. Zhang, Y. C. Lu, M. R. Yuan, Y. H. Xu, Q. Xu, Q. L. Yang, Y. K. Liu, J. Q. Gu, Y. F. Li, Z. Tian, C. M. Ouyang, W. L. Zhang, J. G. Han, *Adv. Optical Mater.* **2022**, *10*, 2102561.
22. X. Liu, Y. Feng, K. Chen, B. Zhu, J. M. Zhao, T. Jiang, *Opt. Express* **2014**, *22*, 20107.
23. Y. T. Zhao, B. Wu, B. Y. Xue, Y. Zhang, Q, Cheng. *Appl. Phys. Exp.* **2019**, *12*, 054005.
24. X. Y. Liu, Y. Lei, X. Zheng, Y. Ren, X. X. Gao, J. J. Zhang, T. J. Cui, *Adv. Mater. Technol.* **2022**, 2200129.
25. L. F. Ye, Z. Y. Wang, J. L. Zhuo, F. Han, W. W. Li, Q. H. Liu, *IEEE Trans. Antennas Propag.* **2022**, *70*, 3237.
26. Z. W. Cheng, H. F. Ma, M. Wang, T. J. Cui, *Adv. Photonics Res.* **2022**, *3*, 2100313.
27. Y. S. Pan, Y. C, Y. D. Dong, *IEEE Trans. Antennas Propag.* **2022**, *70*, 931.
28. H. C. Zhang, L. P. Zhang, P. H. He, J. Xu, Q. Chen, F. J. Garcia-vidal, T. J. Cui, *Light:Sci. Appl.* **2020**, *9*, 1.
29. X. Tian, P. M. Lee, Y. J. Tan, T. Y. Wu, H. C. Yao, M. Y. Zhang, Z. P. Li, K. A. Ng, B. K. Tee, J. S. Ho, *Nat. Electron.* **2019**, *2*, 243.

30. M. Wang, S. Sun, H. F. Ma, T. J. Cui, *IEEE Trans. Microwave Theory Tech.* **2019**, *268*, 732.
31. K. D. Xu, F. Y. Zhang, Y. J. Guo, L. F. Ye, Y. H. Liu, *IEEE Photon. Tech. Lett.* **2020**, *32*, 1431.
32. L. F. Ye, Y. Chen, J. L. Zhou, H. F, Y. Zhang, Q. H. Liu, *J. Phys. D: Appl. Phys.* **2020**, *53*, 235502.
33. H. C. Zhang, T. J. Cui, Q. Zhang, Y. F. Fan, X. J. Fu, *ACS Photonics* **2015**, *2*, 1333.
34. D. J. Hou, J. J. Wu, C. J. Wu, J. Q. Shen, H. L. Chiueh, L. Y. Cheng, H. E. Lin, *Opt. Exp.* **2016**, *24*, 7387.
35. X. X. Gao, H. C. Zhang, P. H. He, Z. X. Wang, J. Y. Lu, R. T. Yan, T. J. Cui, *IEEE Trans. Compon. Packag., Manuf. Technol.* **2019**. *9*, 2267.
36. M. N. Wang, M. Tang, H. C. Zhang, L. P. Zhang, T. J. Cui, J. F. Mao, *IEEE Trans. Compon. Packag., Manuf. Technol.* **2020**, *10*, 1367.
37. H. A. Haus, W. Huang, *Proc. IEEE* **1991**, *79*, 1505.
38. W. P. Huang, *J. Opt. Soc. Am. A.* **1994**, *11*, 963.

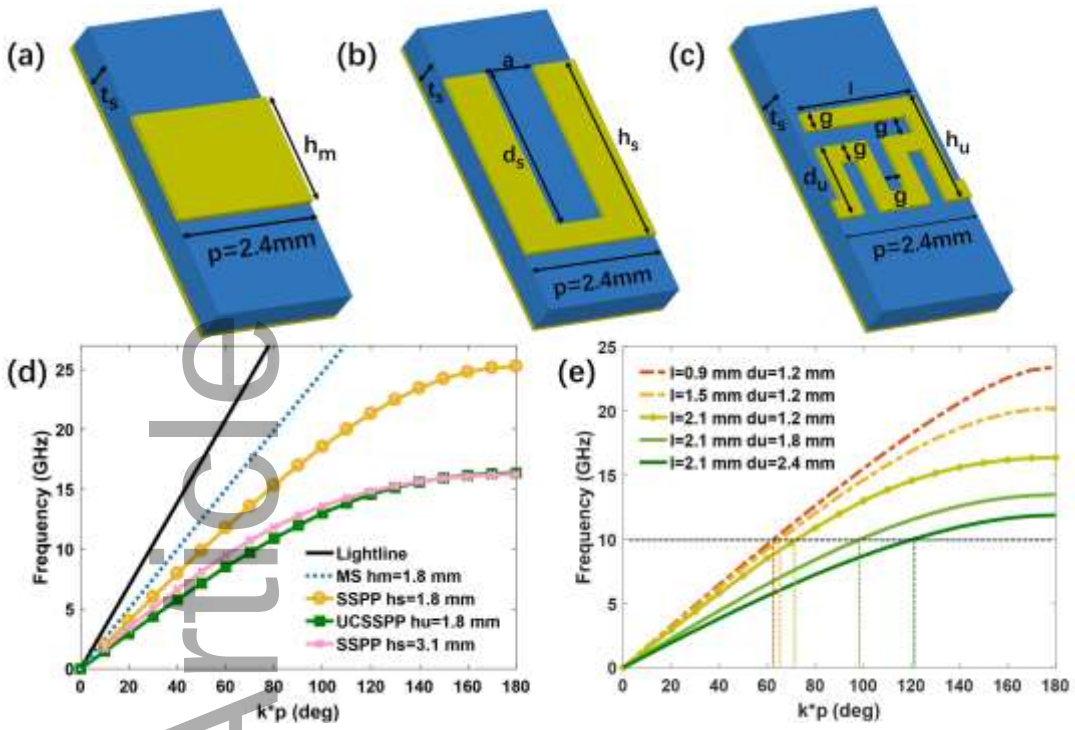

Figure 1. The unit structure of a) MS line, b) conventional SSPP TL, and c) UCSSPP TL. d) Dispersion diagrams of different units, in which p = 2.4 mm, a = 0.9 mm, l = 2.1 mm, g = 0.3 mm. e) Dispersion diagrams of the proposed ultra-compact SSPP unit with different l and d_u.

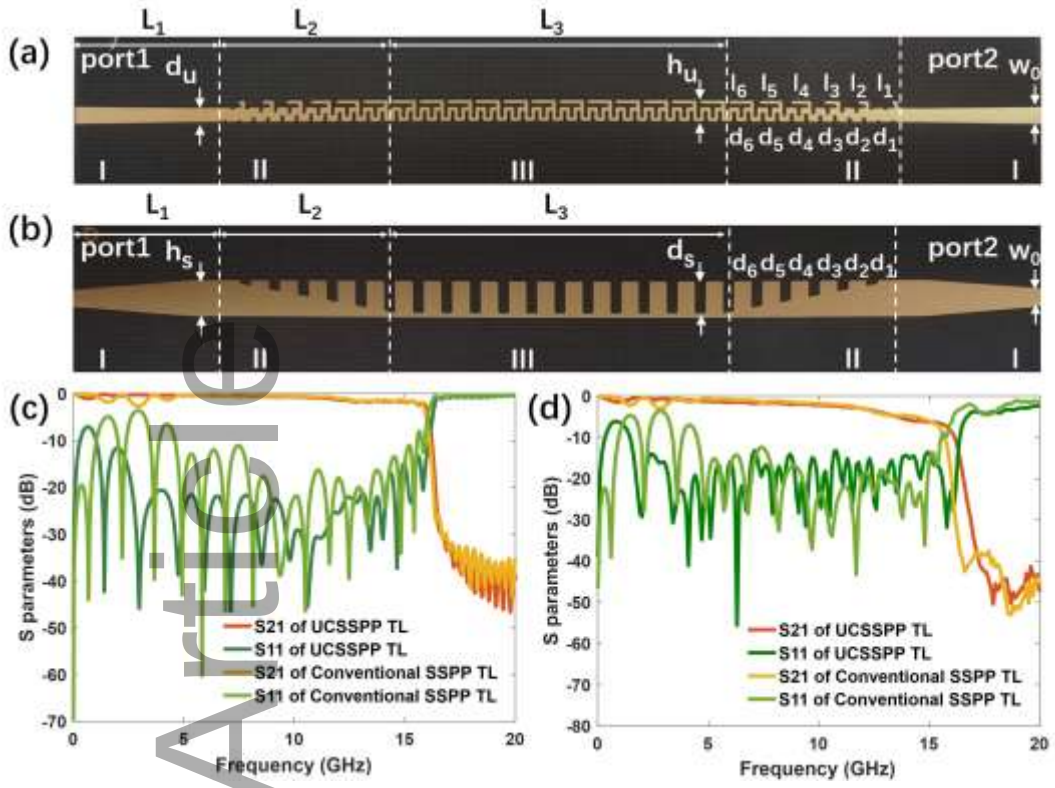

Figure 2. a) The schematic diagrams of UCSSPP TL, in which h_u = 1.8 mm, d_u = 1.2 mm, l_1 = 0.5mm, l_2 = 0.9 mm, l_3 = 1.3 mm, l_4 = 1.65 mm, l_5 = 1.9 mm, l_6 = 2.05 mm, d_1 = 0.15 mm, d_2 = 0.4 mm, d_3 = 0.55 mm, d_4 = 0.7 mm, d_5 = 0.8 mm and d_6 = 0.85 mm. b) The schematic diagrams of conventional rectangular-groove SSPP TL, in which h_s = 3.1 mm, d_s = 2.7 mm, d_1 = 0.3 mm, d_2 = 0.75 mm, d_3 = 1.2 mm, d_4 = 1.65 mm, d_5 = 2.1 mm and d_6 = 2.5 mm. c) The simulated and d) the measured transmission coefficients (S21) and reflection coefficients (S11) of UCSSPP TL and conventional SSPP TL.

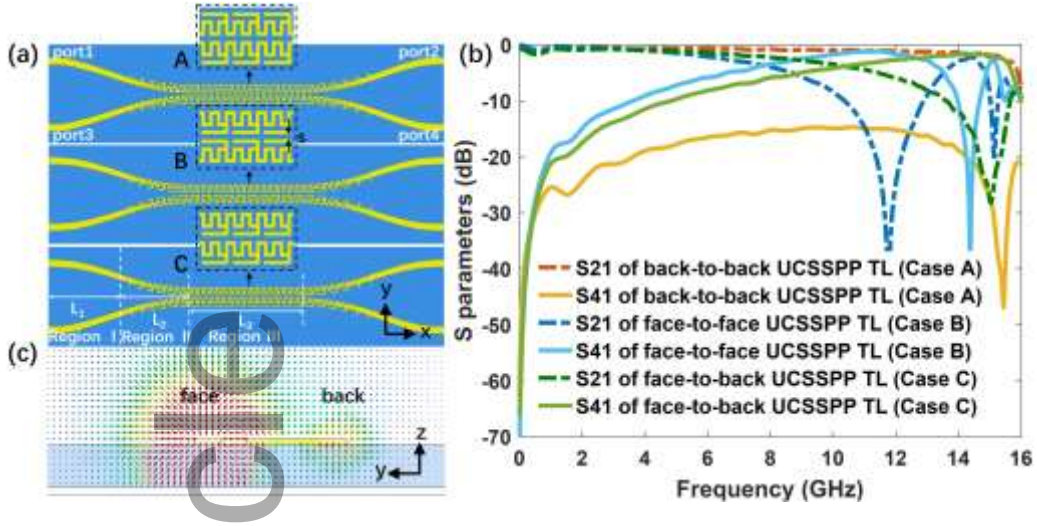

Figure 3. a) Structures of two adjacent UCSSPP TLs arranged in cases A, B and C, in which, L_1 = 18.4 mm, L_2 = 14 mm, L_3 = 38.4 mm and the separation of two UCSSPP TLs is s = 0.4 mm. b) The simulated transmission coefficient (S21) and coupling coefficient (S41) of three cases. c) Simulated electric field vector distribution on the *yoz*-plane of cross section of the UCSSPP unit.

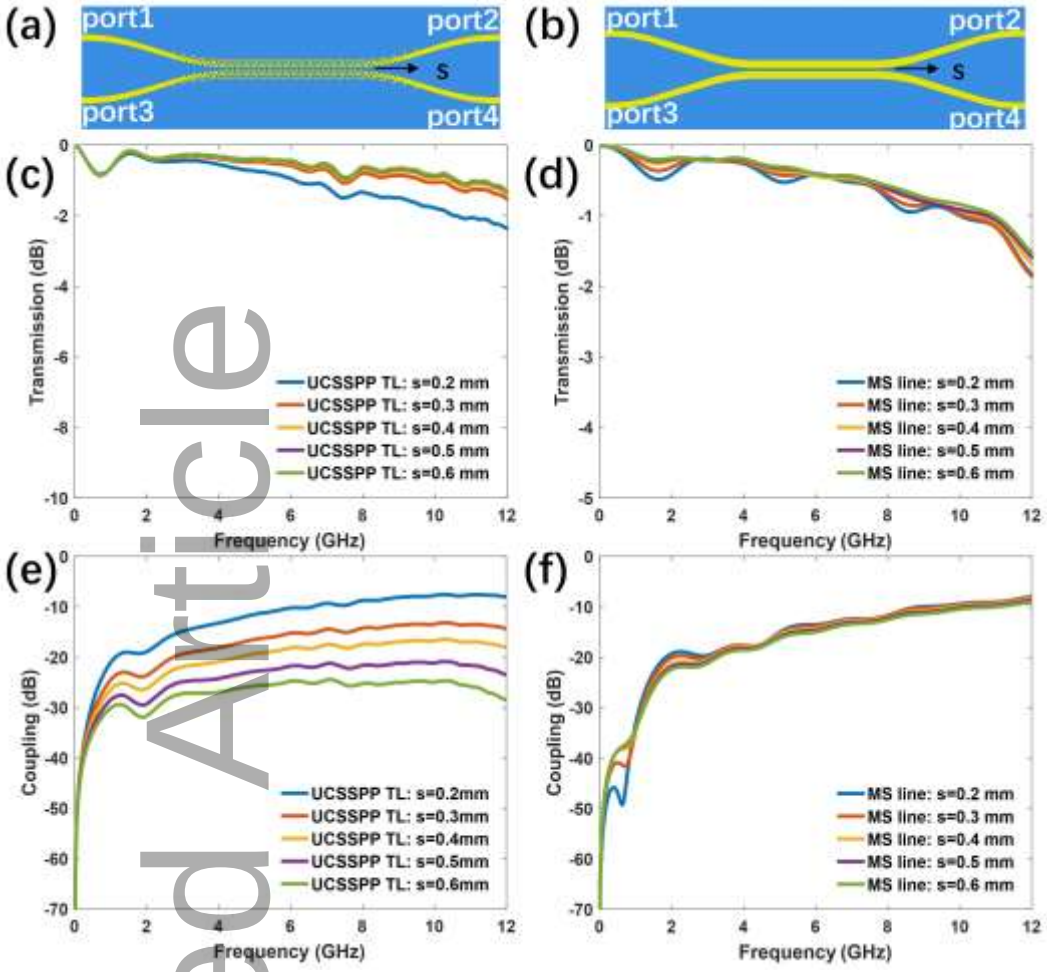

Figure 4. a) The structures of two adjacent UCSSPP TLs in back-to-back case. b) The structures of two adjacent MS TLs. c-f) Simulated S21 and S41 of UCSSPP TLs and MS TLs with different separations.

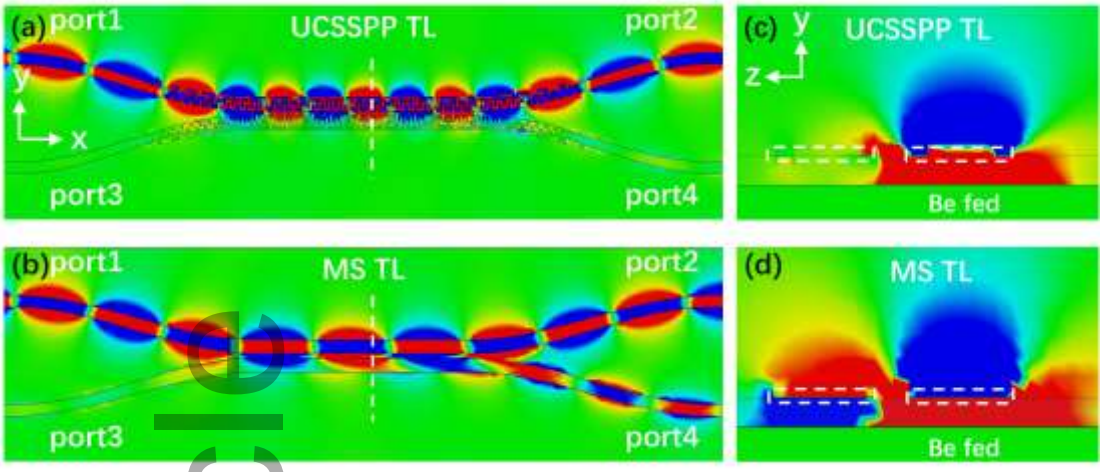

Figure 5. Simulated electric field distributions (E_z) of a) UCSSPP TLs and b) MS TLs on the *xoy*-plane with s = 0.6 mm at 11 GHz. Simulated electric field distributions (E_z) of c) UCSSPP TLs and d) MS TLs on the *yoz*-plane.

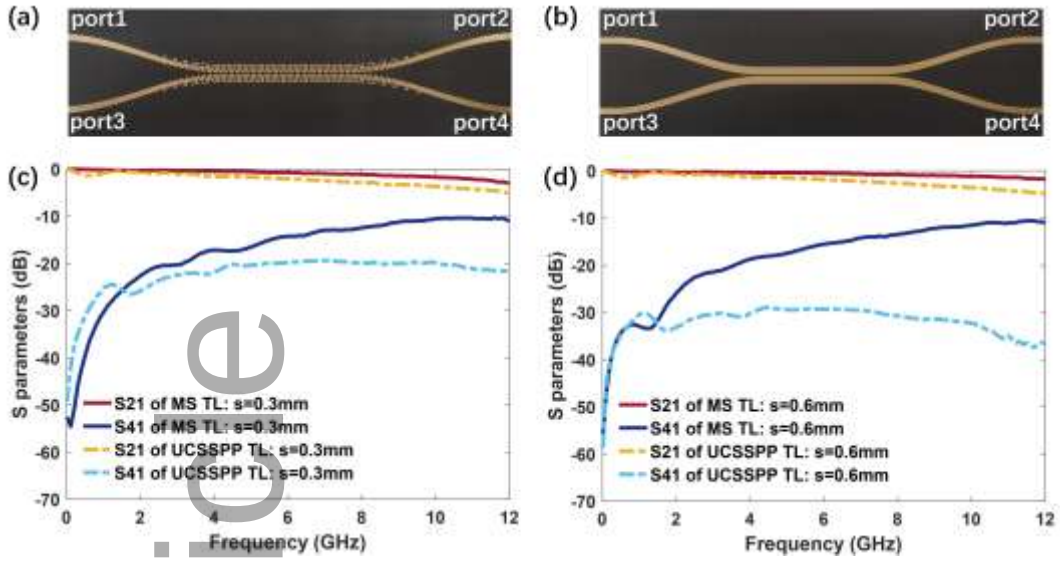

Figure 6. Fabricated samples of a) UCSSPP TLs and b) MS TLs. Measured S21 and S41 of MS TLs and UCSSPP TLs with c) s = 0.3 mm and d) s = 0.6 mm.

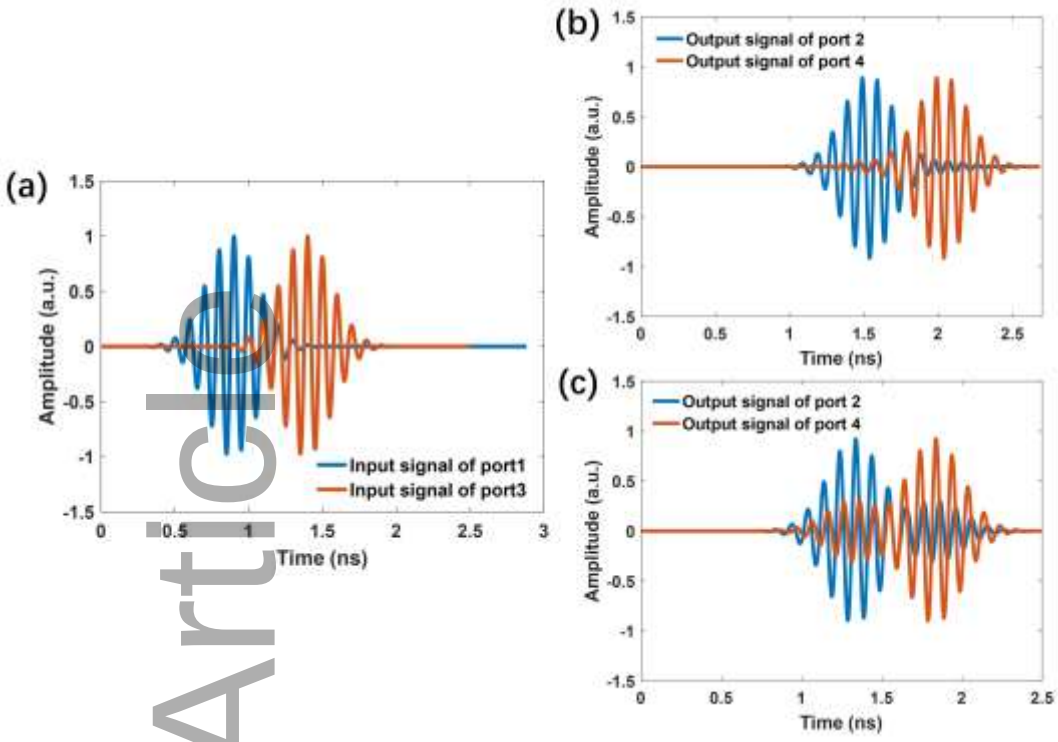

Figure 7. a) The input signals from port 1 and port 3 of broadband Gaussian pulses (8−12 GHz) with a 0.5 ns time interval. The output signals of port 2 and port 4 of b) UCSSPP TLs and c) MS TLs.

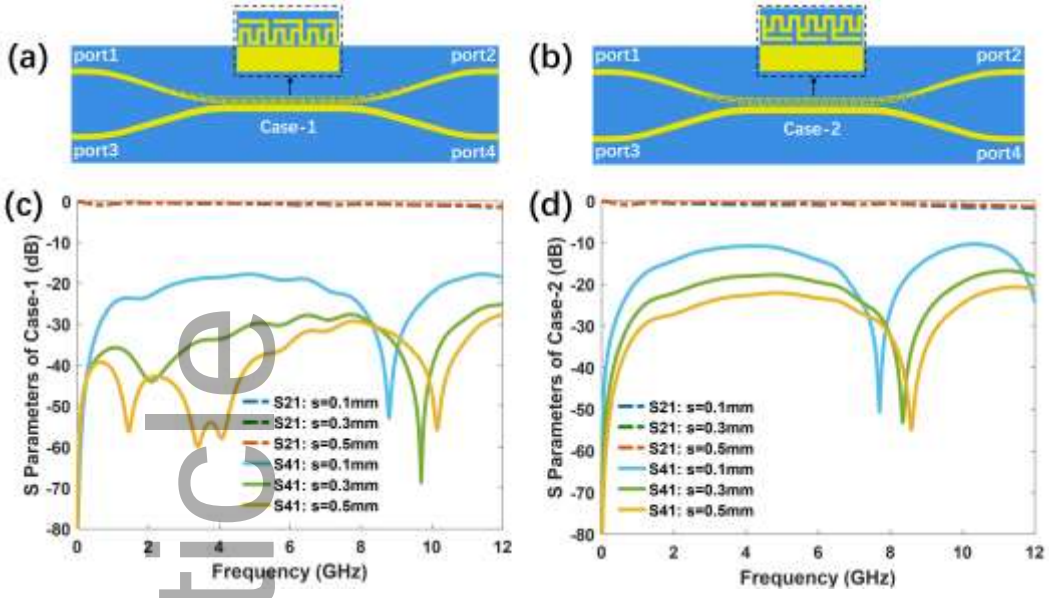

Figure 8. The structure of a) Case-1 and b) Case-2. The simulated S21 and S41 of c) Case-1 and d) Case-2.

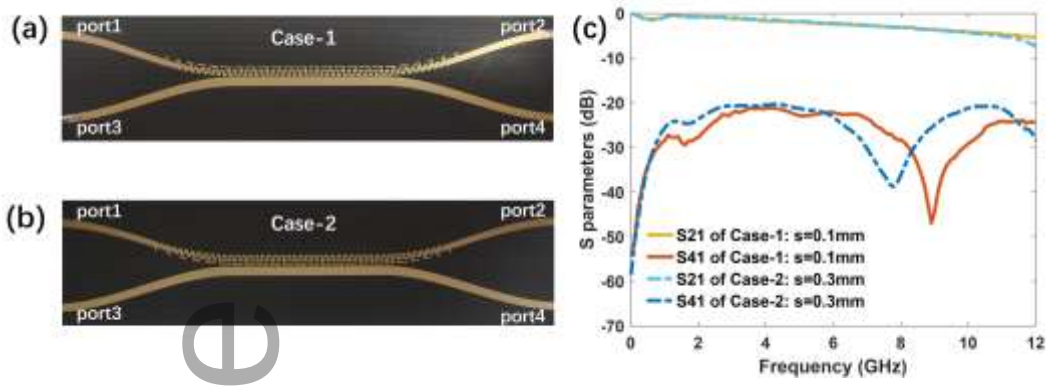

Figure 9. Fabricated samples of a) Case-1 with *s* = 0.1 mm and b) Case-2 with *s* = 0.3 mm. c) Measured S21 and S41 of Case-1 and Case-2.

Table I

COMPARISON BETWEEN UCSSPP TLs AND PREVIOUS WORKS.

Type	Ref	Linewidth (mm)	Separation (mm)	S41 from 0 to 12GHz (dB)	Asymptotic frequency (GHz)
Two SSPP TLs	[26]	2.4	0.8	< -15	15
	This work	**1.8**	**0.6**	**< -28**	**15.8**
SSPP TL & MS TL	[27]	1.2	3.6	< -20	40
	[28]	2.5	0.4	< -10	15.5
	[29]	2.44	2.4	< -20	16
	This work	**1.8**	**0.1**	**< -30**	**15.8**

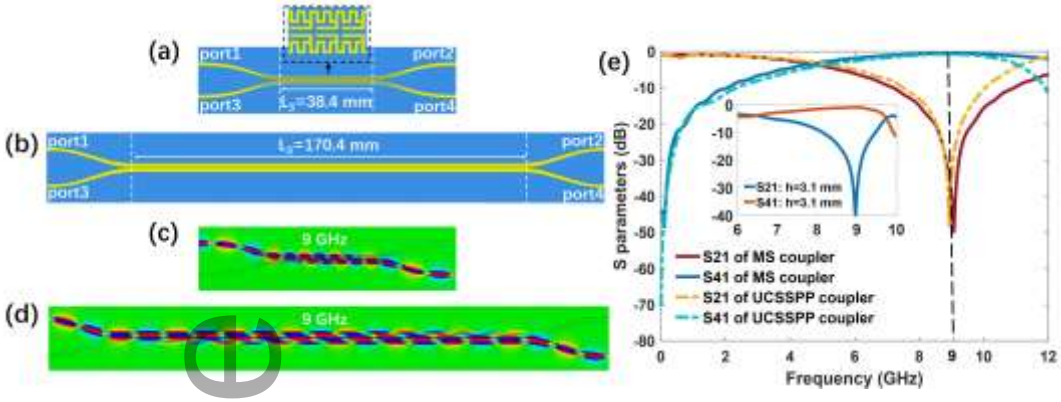

Figure 10. The structure of a) UCSSPP coupler and b) the MS coupler, in which $h_u = h_m = 1.8$ mm, $s = 0.2$ mm. The electric field distributions (E_z) on the *xoy* plane at 9 GHz of c) UCSSPP coupler and d) MS coupler. e) Simulated S parameters of the two couplers, and the inset is the simulated S parameters of the UCSSPP coupler with $h_u = 3.1$ mm, $s = 0.2$ mm and $L_3 = 19.2$ mm.

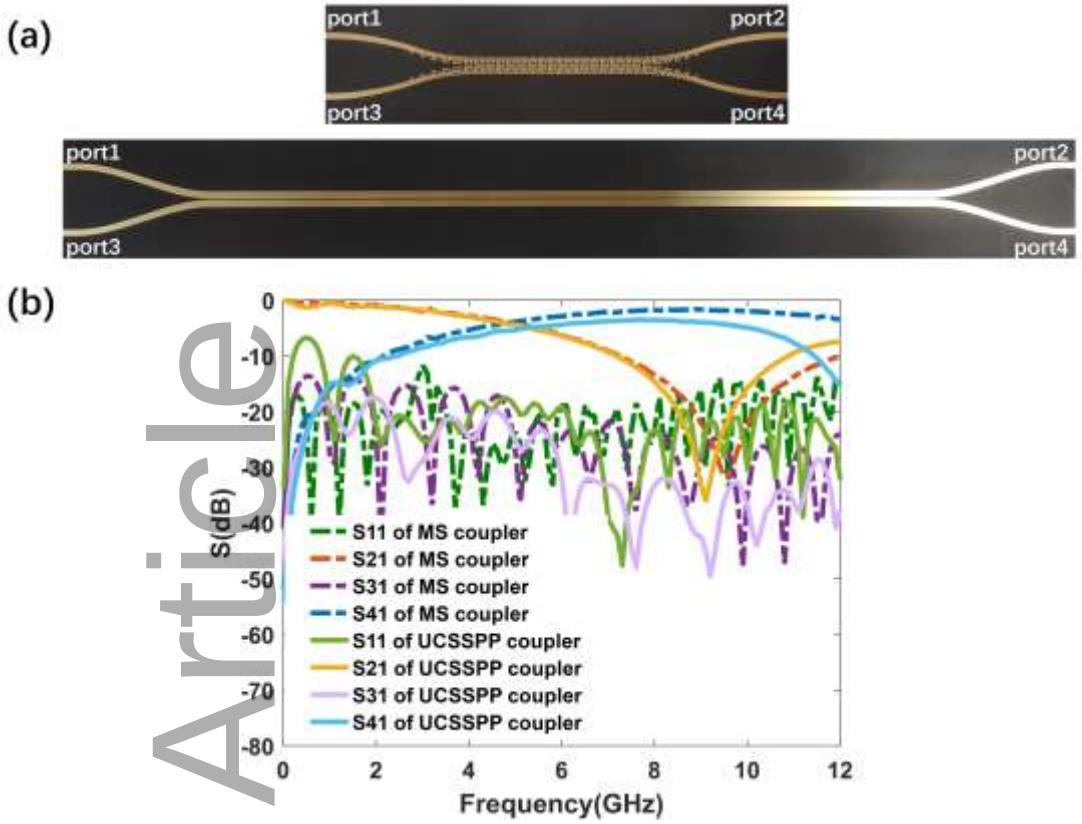

Figure 11. a) The fabricated samples of the UCSSPP coupler and MS coupler. b) Measured S parameters of two couplers.

An ultra-compact spoof surface plasmon polariton (UCSSPP) transmission line (TL) that can achieve great linewidth reduction is proposed, and the coupling effects between two UCSSPP TLs under different arrangements are further studied. The results show that the proposed UCSSPP TL has significant advantages in linewidth reduction, crosstalk suppression, device miniaturization design, and so on.